Geoscience Frontiers 12 (2021) 746–755

Contents lists available at ScienceDirect

Geoscience Frontiers

journal homepage: www.elsevier.com/locate/gsf

Research Paper

Volcanic emissions and atmospheric pollution: A study of nanoparticles

Erika M. Trejos [a], Luis F.O. Silva [b,*], James C. Hower [c,d], Eriko M.M. Flores [e], Carlos Mario González [a], Jorge E. Pachón [f], Beatriz H. Aristizábal [a]

[a] Hydraulic Engineering and Environmental Research Group, Universidad Nacional de Colombia Sede Manizales, Manizales, Colombia
[b] Department of Civil and Environmental, Universidad de la Costa, Calle 58 #55-66, Barranquilla 080002, Colombia
[c] University of Kentucky, Center for Applied Energy Research, 2540 Research Park Drive, Lexington, KY 40511, USA
[d] Department of Earth & Environmental Sciences, University of Kentucky, Lexington, KY 40506, USA
[e] Universidade Federal de Santa Maria, Santa Maria, Brazil
[f] Centro Lasallista de Investigación y Modelación Ambiental – CLIMA, Universidad de La Salle, Bogotá, Colombia

ARTICLE INFO

Article history:
Received 4 June 2020
Received in revised form 11 August 2020
Accepted 26 August 2020
Available online 02 October 2020

Keywords:
Nanoparticles
Amorphous phases
Potential hazardous elements
Road dust
Volcano zone

ABSTRACT

The influence of emissions of an active volcano on the composition of nanoparticles and ultrafine road dust was identified in an urban area of the Andes. Although many cities are close to active volcanoes, few studies have evaluated their influence in road dust composition. Air quality in urban areas is significantly affected by non-exhaust emissions (e.g. road dust, brake wear, tire wear), however, natural sources such as volcanoes also impact the chemical composition of the particles. In this study, elements from volcanic emissions such as Si > Al > Fe > Ca > K > Mg, and Si—Al with K were identified as complex hydrates. Similarly, As, Hg, Cd, Pb, As, H, Cd, Pb, V, and salammoniac were observed in nanoparticles and ultrafine material. Mineral composition was detected in the order of quartz> mullite> calcite> kaolinite> illite> goethite> magnetite> zircon> monazite, in addition to salammoniac, a tracer of volcanic sources. The foregoing analysis reflects the importance of carrying out more studies relating the influence of volcanic emissions in road dust in order to protect human health. The road dust load (RD_{10}) ranged between 0.8 and 26.8 mg m^{-2} in the city.

1. Introduction

Air quality in urban areas has suffered great pressure in recent years due to various anthropogenic activities (demolition/construction, industries, vehicles, biomass burning, among others), with the increase in the vehicle rate one of the main causes discussed by different authors (Bergbäck et al., 2001; Sörme et al., 2001; EEA, 2004; Amato et al., 2009, 2011; González, 2017). Natural sources, such as sea spray, vegetation, and volcanoes can increase pollution levels (Silva et al., 2020). There are suggestive hypotheses that these particles of natural sources may have a greater potential for adverse health impacts compared with their larger counterparts (WHO, 2016). Long-term exposure studies would be required to confirm these hypotheses, but these are currently unavailable (Silva et al., 2020).

Particulate matter is one of the pollutants of most concern due to its effects on human health and its complex and varied composition, shape and size (PM_{10}, $PM_{2.5}$, ultrafine, and nanoparticles) (WHO, 2016). These effects ranging from respiratory to cardiovascular diseases, cognitive decline, and stroke (Kioumourtzoglou et al., 2016; WHO, 2016; Chen et al., 2017; Saikia et al., 2018; Ramírez et al., 2019). Metals, such as Zn and V have been associated with cardiovascular diseases, whereas Ni, Si, and Ti are related with respiratory exacerbations (Stafoggia and Faustini, 2018). Organic compounds, including PAHs, are highly toxic and involved in carcinogenic processes (Grigoratos and Martini, 2015).

The contribution of vehicular sources to particulate matter emissions are exhaust-type (exhaust pipe) and non-exhaust-type (brake wear, tire wear, and road dust) The particles emitted by the exhaust gases and the wear of the vehicle parts, together with primary and secondary particles of anthropogenic and natural origin, are deposited and accumulate daily on the pavement as road dust (Amato et al., 2009, 2011). The action of passing vehicles causes re-suspension of road dust with an aerodynamic diameter of less than 10 μm (RD_{10}) due to turbulence generated by the wheels. The importance of RD_{10} emissions resides in that they can be comparable with non-depleted emissions as different studies have found (Amato et al., 2009, 2011; Bukowiecki et al., 2010; Harrison et al., 2008; Querol et al., 2001). Ultra-fine particles smaller than 300 nm diameter contribute over 99% of total particulate emissions (Kumar et al., 2009). Unlike the lower cut-off size, any upper cut-off size over 300 nm does not influence ultrafine particles (UFPs) estimates greatly. In Europe, the contribution from road traffic varied from ~32% of total nanoparticles (PNs) emissions in Greece to ~97% in Luxemburg. France, Spain, Germany, Italy, UK and Poland are

* Corresponding author.
E-mail addresses: felipeqma@hotmail.com (L.F.O. Silva), bharistizabalz@unal.edu.co (B.H. Aristizábal).

https://doi.org/10.1016/j.gsf.2020.08.013

the top six PN emitters in the European Union and together, their road traffic contributes nearly 3/4 (~72%) of the total traffic-induced PN emissions in the European Union (Kumar et al., 2014). Road dust emissions vary widely in quantity and chemical composition at each location, as they are influenced by different parameters, including road characteristics, traffic condition, land use, and meteorology (Amato et al., 2009, 2011; Pachón et al., 2020), in addition, the contribution by other emission sources. The influence of other variables, such as volcanism in road dust levels is yet to be investigated. Currently the current estimation models lack sufficient experimental information on the impact of the different factors that control this variability (Amato et al., 2013).

Studies have documented the impact of volcanoes on air quality, observing large ambient SO_2 concentrations downwind from volcano plumes (Carn et al., 2011; Carn et al., 2017; Longo, 2013; Cuesta et al., 2018; Cuesta et al., 2020). Volcanos can deliver large number of particles from nano (<50 nm) to coarse PM_{10} to the atmosphere (Buseck and Adachi, 2008; Schäfer et al., 2011; Businger et al., 2015, Silva et al., 2020).

Mineral dust and particulate material from volcanic emissions differ significantly due to the generation processes. The first corresponds to the dust deposited on the surface of the pavement and passes into the air through the action of external agents (vehicular passage, air, among others). The second corresponds to magma produced by a volcanic eruption and fragments (Malek et al., 2019). The re-suspended dust is composed of several types of minerals, such as silica, clay, micas, feldspar, carbonates, sulfates, and phosphates. In contrast, the particulate material from volcanic emissions is generally composed of silica (vitreous glass, quartz, and other polymorphs) and plagioclase feldspar (solid-solution series from Na- to Ca-feldspar) (Malek et al., 2019). In order to identify mineral components and hazardous elements in road dust, electron microscopy techniques have become widely available. Field emission scanning electron microscopy (FE-SEM) and high-resolution transmission electron microscopy (HR-TEM) observations coupled to energy dispersion X-ray spectroscopy (EDS) give physicochemical information of the individual particles, allowing the distinction of contribution sources (Labrada et al., 2012; Malek et al., 2019; Mantovani et al., 2018; Onat et al., 2013).

Colombia has many volcanoes, some of the most active are Nevado del Ruiz, Nevado del Huila, and Galeras. The Nevado del Ruiz volcano is located 28-km southeast of the city of Manizales, could reach a VEI (Volcanic Explosivity Index) of 3–4 (SGC, 2015) and registering permanent activity of daily SO_2 emissions (SGC, 2019). In a study carried out in 2015 by Carn et al. (2017) the Nevado del Ruiz volcano was the fifth highest annual emitter in Latin America with SO_2 emissions of 1145 kt in 2015 (above the volcanoes: Popocatepetl volcano in Mexico, Nevado del Huila volcano in Colombia, Tungurahua volcano in Ecuador, Ubinas volcano and Sanbancaya volcano in Peru). The region where the city of Manizales is located has been characterized in geological and environmental samples, including rocks, soil, water, etc. for presenting volcanic soils (Erazo et al., 2015; Laj and Boutron, 1990; Parnell and Burke, 1990). Likewise, Nevado del Ruiz plume emissions can impact Manizales air quality (Cuesta et al., 2018, 2020). In fact, large sulfate concentrations related to volcanic ash emissions have been observed in the PM_{10} chemical composition (Velasco, 2015). Furthermore, volcanic SO_2 plume and ash emissions are associated with acid rain in Manizales (González and Aristizábal, 2012). A rain profile of sulphates> calcium> chloride> nitrates concentration has been found (González and Aristizábal, 2012).

In this study, the influence of emissions from the Nevado del Ruiz volcano on the composition and morphology of nanoparticles (NPs - particles with aerodynamic diameter < 50 nm) and ultrafine particles (UFPs - particles with aerodynamic diameter < 100 nm) of road dust in the city of Manizales was determined by applying advanced electron microscopy techniques (FE-SEM/EDS and HR-TEM/EDS). This study is the first of its kind in Latin America, a region with severe air pollution problems and numerous active volcanoes.

2. Methodology

2.1. Area of study

Manizales is a medium-size Andean city, located in the central west of Colombia on the western slope of the Cordillera Central (altitude of 2150 m.a.s.l - meters above sea level) (Cuesta et al., 2020). The urban region has an approximate area of 54 km^2 with an urban population of 405,234 inhabitants (DANE, 2019). The city has a population density of ~7504 inhabitants per km^2 in the urban area and it is the second city in the country with the highest motorization rate (455.2 vehicles per 1000 inhabitants in the year of 2018) above Bogotá and Medellín (329 and 454 vehicles/1000 inhabitants in the year of 2018) (González, 2017; Manizales Cómo Vamos, 2019). The city's vehicle fleet is conformed of 169,142 vehicles for the year 2017, 95.4% of which correspond to private vehicles (vehicular activity: 25 km/day/vehicle) and motorcycles (vehicular activity: 25 km/day/vehicle) (Unal-Corpocaldas, 2019). The remaining 4.6% corresponds to taxis, buses and trucks. The city has three peak traffic periods: (1) 06:30 to 07:30 h. (2) between 11:45–12:45 h; and between 13:30–14:30 h. (3) 17:30 to 18:30 h (Findeter, 2017).

The city is characterized by having microclimates of precipitation, with annual precipitation of approximately 1454 mm, 1670 mm, and 1776 mm for the eastern, central, and western areas, respectively. The diurnal temperature profile ranges between 12 and 24 °C, maximum solar radiation of 1306 W m^{-2}, high relative humidity between 82%, and low wind speeds ≤2 m s^{-1}. Valley-mountain wind circulation patterns are characterized as ascending by day and descending by night (as a result of heating and cooling by radiation) with possible transport of volcanic emissions during downslope wind (Fig. 1A) (Cuesta et al., 2020; González, 2017). Low wind speeds along with wind patterns generate minimal dispersion of pollutants and are directed towards the urban area of the city (Cuesta et al., 2020; González, 2017). Furthermore, the high precipitation favors the washing of the atmosphere, dragging the particulate material of the air, this phenomenon is known as Scavenging (González and Aristizábal, 2012). These particular characteristics can generate pressure on air quality of the city, with episodes of contamination during low rain seasons with potential impact on the population and natural ecosystems (Unal-Corpocaldas, 2019).

Local atmospheric chemistry is influenced by the proximity to the Nevado del Ruiz volcano, the fifth most active in Latin America, registering significant activity since 2010 with daily SO_2 and ash-emission episodes (Fig. 1B) (Carn et al., 2017). During the sampling period (July–September of 2019) height of emission column was reported between 636 and 1300 m (SGC, 2019).

2.2. Road dust sampling

The RD_{10} samples were taken at 21 points distributed across the urban area of Manizales (Fig. 2). The field campaign was conducted between July and September of 2019 during dry season (9-mm accumulated precipitation and average temperature of 18 °C) as established by the sampling method described by Amato et al. (2009, 2011). It was carried out in the dry season because during this time it is a critical condition where the resuspension of RD_{10} is higher than during the rain period. A “dry dust sampler” equipment designed at the Spanish Research Council was used; a description of the instrument is available elsewhere (Amato et al., 2009, 2011).

A pavement section of the active right lane was chosen at a distance of 1 m from the gutter and without episodes of rain in the previous 24 h of each sampling. An area of 1 m^2 was sampled for 30 min with an air flow of approximately 30 L min^{-1}. At each site, sampling was performed 3 times using three different filters to reduce occasional errors and to

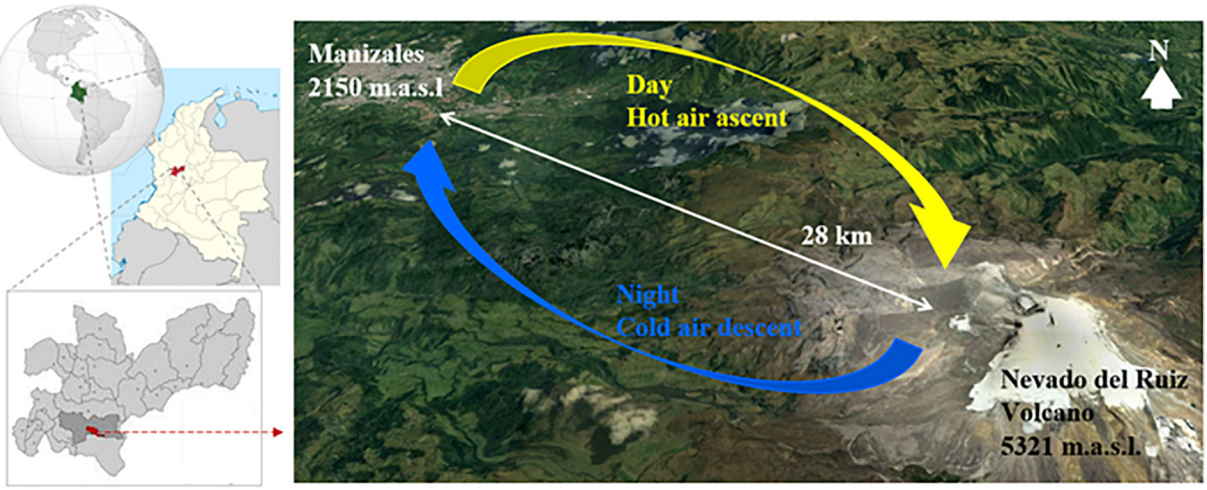

(a)

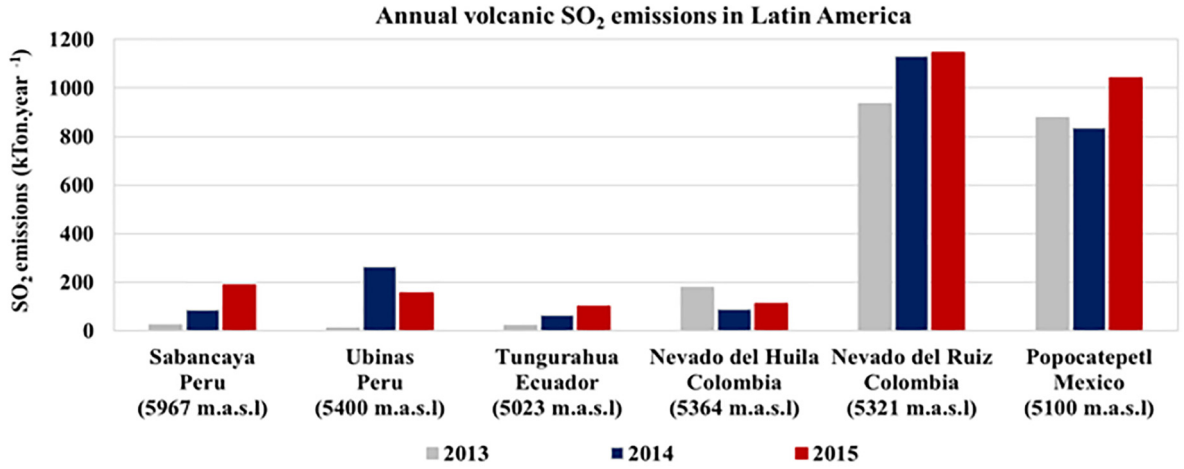

(b)

Fig. 1. (A) Location of Manizales in the Colombian Andean region. (B) Annual SO_2 emissions comparison among volcanoes with similar altitude in Latin America (Carn et al., 2017).

collect enough samples for analysis. Samples were collected on a glass fiber filter Whatman ® brand (47 mm Ø). Filters were dried at 500 °C for 12 h and dehumidified for 48 h (at 22 °C and 50% of relative humidity). After sampling, the filters were kept dried for 48 h (at 22 °C and 50% of relative humidity) and then refrigerated at 4 °C until before the FE-SEM/EDS and HR-TEM/EDS analysis. During each 48 h conditioning two weighing procedures were carried out every 24 h, in each the filter mass was measured three times using a microbalance (Mettler Toledo MS205DU). The road dust mass fraction per m^2 (RD_{10} load) at each site was calculated by difference in weights before and after sample collection, and averaging the mass collected in the 3 samples (mg m^{-2}).

2.3. Morphological analysis

To investigate the NP and the UFP, a random filter was selected from the three sampled by each site. In total, 21 RD_{10} samples were analyzed. To ensure adequate reliability of results, all laboratory materials were maintained for 24 h in a 15% *v*/v nitric acid bath and washed with Milli-Q H_2O prior to use to prevent possible adulteration that could modify the results (Gredilla et al., 2017; Gredilla et al., 2014). In the laboratory, sampled condensed water and precipitate particles were evaluated in two ways: (1) 1 mL of sampled water was pipetted onto the Cu-grid of the field emission scanning electron microscope (FE-SEM), and high-resolution transmission electron microscope (HR-TEM) stub; (2) the decanted particles were sampled separately and suspended in water again by ultrasound, to later be transferred and analyzed with advanced microscopes. In some cases, it was necessary to wait up to 48 h for the water to evaporate before the samples could be analyzed. However, this methodology was chosen to avoid chemical, mineralogical, morphological, and geo-metric modifications of NPs and UFPs. This procedure was established based on published studies (Ribeiro et al., 2010).

The mineralogy of NPs and UFPs were performed using a Field Emission Scanning Electron Microscope (FE-SEM), Zeiss model FEG sigma 300 VP with a X Flash Detector 410-M (Civeira et al., 2016a) and advanced High-Resolution Transmission Electron Microscope (HR-TEM, 200 kV) equipped with an Energy-Dispersive X-ray Spectrometer (EDS). Electron diffraction patterns of the crystalline phases were recorded in selected area electron diffraction (SAED), micro-beam diffraction (MBD), and Fast Fourier Transform (FFT) (Silva et al., 2020). In order to facilitate the identification of amorphous, crystalline, oxidized, and sulfate particles, the sequential extraction previously developed by Ribeiro et al. (2010); Ribeiro et al. (2013a); Ribeiro et al. (2013b) was implemented.

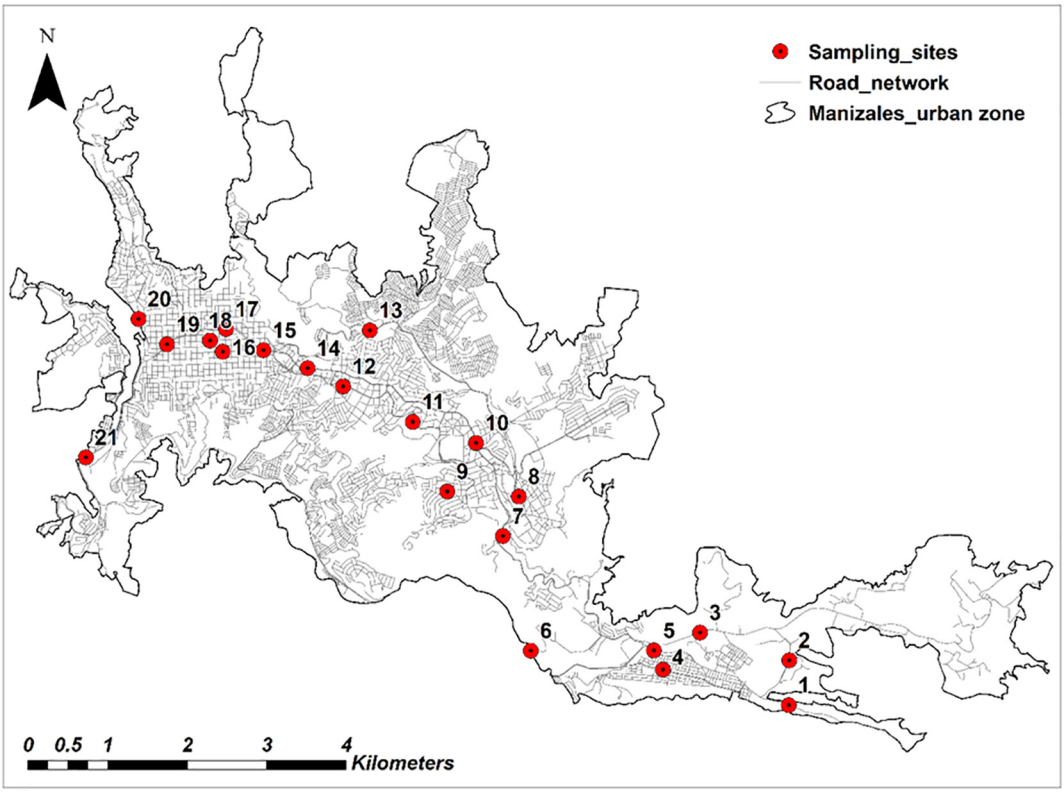

Fig. 2. Location of the RD_{10} load sampling points in Manizales city.

Before FE-SEM and STEM analysis, the HR-TEM specimen holder was cleaned with an Advanced Plasma System (Gatan Model 950) to minimize contamination. The samples were prepared by a critical point dryer on a glass plate, which was mounted on a SEM stub (Cutruneo et al., 2014). The samples were then covered with a thin Au layer (~20 nm) to make it conductive, and a Pt layer to protect the surface. Then, a large and deep rectangular trench was dug in each sample, by rough milling with an ion current of 93 nA at 30 kV. Then, the surface of the cut was polished with an intermediate current of 0.28 nA, using the option "cleaning cross-section". In this option, the ion beam moves in and slices the sample in a direction that is perpendicular to the cut surface. Finally, to attain a fine polish, we used an ion beam with very small aperture and very low current (28 pA), even though it is time-consuming, it was required to avoid artifacts induced by heating. Then, the images were recorded using the Through Lens Detector (TLD), which gives a spatial resolution in a nanometer range. During thinning, the SEM images were subjected to a secondary electron detector to control the process and choose the side that required to be thinned and with an in-lens back-scattered electron detector to distinguish particles using chemical contrast. Finally, the amorphous material re-deposited by the plasma during thinning was removed by scanning the sectioned with a 5 kV ion beam at an angle of 4°–7° with the section surface. In addition, the utilized SAED and nanobeam diffraction patterns were recorded on FEI G2 20 and Philips CM30 TEM. At 200 and 300 kV, amorphization by radiation damage to quartz (but not Fe-bearing minerals) was fast enough to permit SAED and nano-beam diffraction on mineral crystallites and amorphous nano-particles without interference by the quartz matrix. The aperture- selected areas are outlined by a circle in the SAED figures.

Scanning transmission X-ray microscopy was used to perform high spatial resolution (25 nm) spectromicroscopic analysis at the car- bon K-edge (energy range 270–320 eV) to image the distributions of special minerals (e.g., carbonates) and organic matter and identify carbonates in X-ray absorption near-edge spectroscopy spectra (Lepot et al., 2017). The utilized microscope chamber was evacuated to 100 mTorr after sample insertion and back-filled with He. The spectral resolution of 0.8 eV between 275 and 283 eV, 0.15 eV between 283 and 295 eV, 0.5 eV between 295 and 310 eV and the counting times of the order of a few milliseconds or less per pixel were used. The details of data acquisition, processing, and interpretation have been provided by Alleon et al. (2016). Carbonate maps were obtained by subtraction of the X-ray transmission images recorded at 290.3 eV to 285.4 eV (aromatic absorption maximum), and aromatic carbon maps were obtained by subtraction of X-ray transmission images at 285.4 eV (aromatics) to 275 eV (Lepot et al., 2017).

3. Results and discussion

3.1. Road dust load (RD_{10}) variation

RD_{10} load values in Manizales varied between 0.8 and 26.8 mg m^{-2} (Table 1), slightly lower than values obtained in Bogotá (range 1.8–45.8 mg m^{-2}) using the same dust sampler (Pachón et al., 2020). RD_{10} levels were also similar to Zurich, Switzerland (0.2–1.3 mg m^{-2}), Barcelona (3.7–23.1 mg m^{-2}), and Girona, Spain (1.3–48.7 mg m^{-2}) (Amato et al., 2011). It should be noted that these cities do not have proximity to volcanic sources. Studies of this type are focused on determining the relationship between the RD load and the characteristics of the sampling area such as type of paving, traffic intensity, proximity to the braking zone, vegetation, seasonal effects and contribution of anthropogenic sources (Amato et al., 2009, 2011; Hussein et al., 2008; Pachón et al., 2020).

3.2. Chemical and morphological analyses of road dust

The geochemical composition of more than half of road dust load samples detected by EDS presented Fe, Ti, Al-Si-K hydrated complexes, As, Hg, Cd, Pb, and salammoniac (Fig. 3). A similar geochemical profile

Table 1
RD_{10} load estimated in the city of Manizales.

Point No.	Longitude	Latitude	Sampling date	RD_{10} load (mg m^{-2})
1	5.02794°N	−75.45139°W	02/09/2019	26.75
2	5.03301°N	−75.45135°W	20/08/2019	11.72
3	5.03614°N	−75.46143°W	02/09/2019	0.77
4	5.03195°N	−75.46563°W	31/07/2019	8.54
5	5.03413°N	−75.46665°W	30/08/2019	2.52
6	5.03386°N	−75.48126°W	28/08/2019	1.74
7	5.04704°N	−75.48372°W	09/08/2019	1.96
8	5.05149°N	−75.48191°W	08/08/2019	7.19
9	5.05206°N	−75.49001°W	28/08/2019	2.22
10	5.05754°N	−75.48675°W	09/08/2019	2.72
11	5.05992°N	−75.4939°W	30/08/2019	3.17
12	5.06392°N	−75.50177°W	20/08/2019	2.73
13	5.07024°N	−75.49876°W	22/08/2019	3.57
14	5.06598°N	−75.5058°W	06/08/2019	6.46
15	5.06801°N	−75.51079°W	22/08/2019	1.43
16	5.06783°N	−75.51538°W	01/08/2019	7.14
17	5.07040°N	−75.51501°W	28/08/2019	4.16
18	5.06910°N	−75.51682°W	06/08/2019	5.92
19	5.06866°N	−75.52168°W	08/08/2019	6.52
20	5.07151°N	−75.52493°W	01/08/2019	7.53
21	5.05591°N	−75.53086°W	06/08/2019	5.03

was identified in rural background PM_{10} in Colima, Mexico, located 35-km from the "Volcán del Fuego" (Campos et al., 2011) and in other studies (Cangemi et al., 2017; Fernández et al., 2012; Lieke et al., 2013). This profile suggests the influence of the Nevado del Ruiz volcano in the city. In fact, during the sampling period the prevailing winds came from the southeast direction, corresponding to the area where the volcano is located (Fig. 4 and Table 1). Likewise, episodes of volcanic ash emission occurred as discussed in section 2.1.

Through the SEM images, the morphology of the particles (size and shape) was observed. Multiple shapes were observed due to the variety of RD_{10} sources, particles with spherical and angular shapes in micrometric and nanometric sizes (Fig. 5). Not only was the shape heterogeneous but also the chemical and mineralogical composition, the minerals detected in the samples were quartz, mullite, calcite, kaolinite, illite, goethite, magnetite, zircon, monazite (Fig. 3A), with size variation between 0.1 nm to 16 μm (Fig. 5). Some of the particles were minerals, as in the case of monazite, but in most of the cases, they were complex particles containing both amorphous and crystalline material, as characterized by HR-TEM/EDS (Fig. 3A). Fig. 6 shows the classic example of the complexity of such particles, especially when they are incipient welding facies of road dust near volcano area. Similar particles were detected by Alarcón et al. (2020) in a study of the Cerro Bravo volcano from a solid deposit of pyroclastic ash flow using SEM. The Cerro Bravo volcano is located approximately 25 km from Manizales; however, the most recent

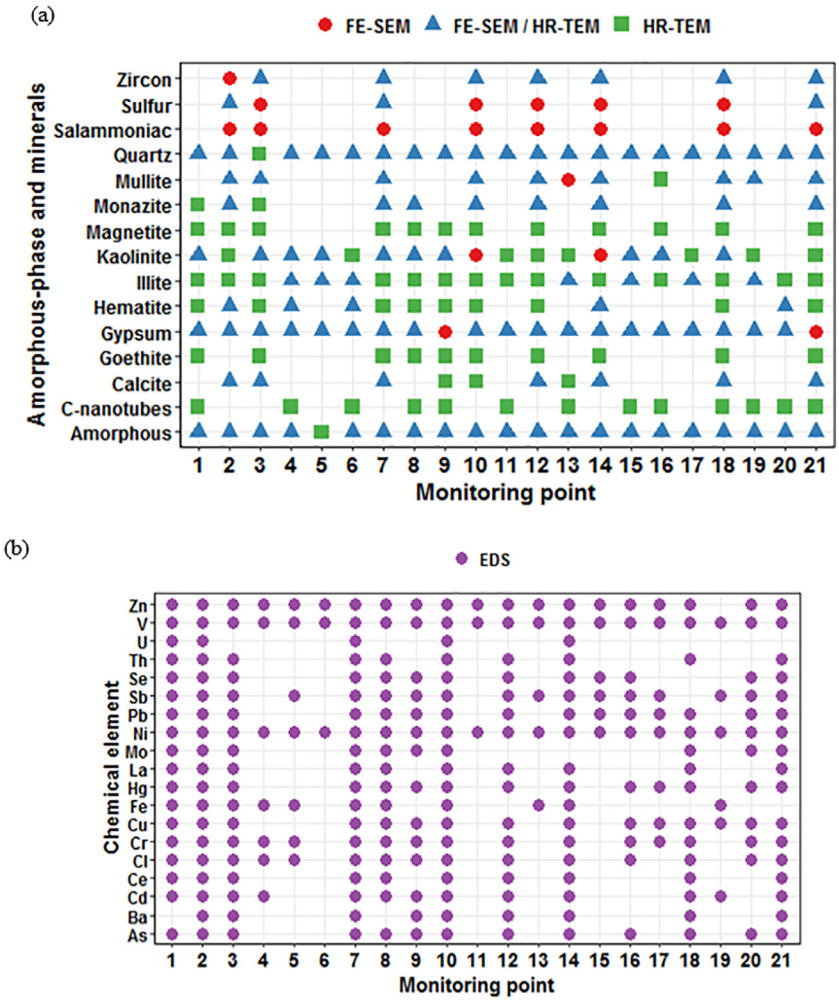

Fig. 3. (A) Amorphous phases, minerals, and (B) particles chemical composition from studied road dust by FE-SEM, HR-TEM, and EDS. Other elements found were S, Al, Si, Ca, K, Na, Mn, and Mg.

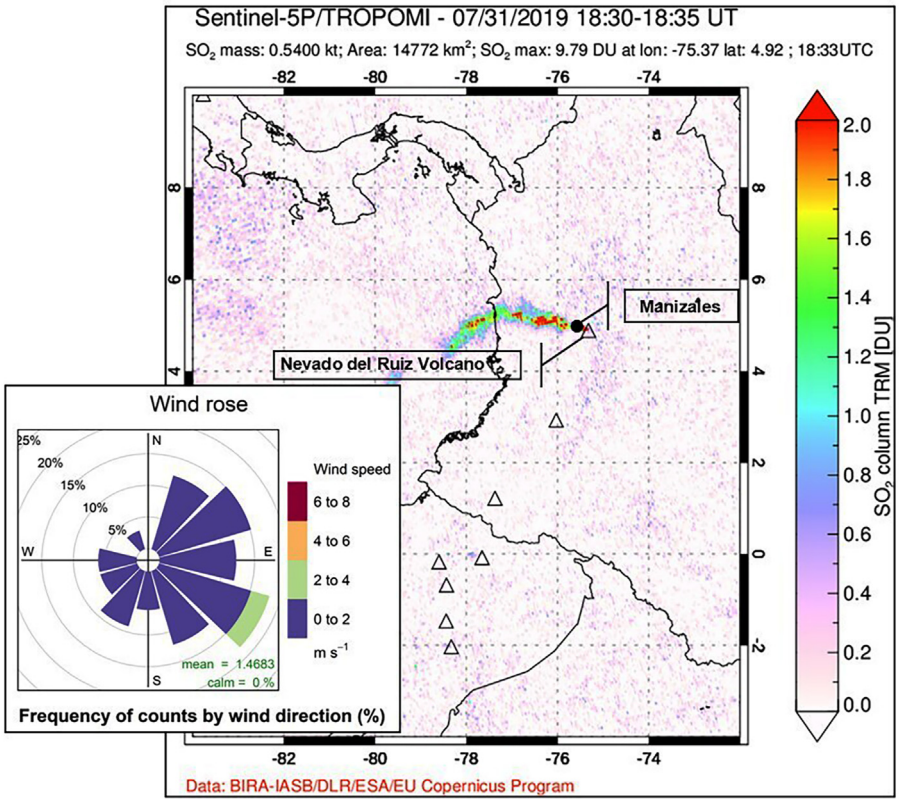

Fig. 4. TROPOMI satellite image of the emission of volcanic ash, trajectory and height of the SO_2 column during a sampling day (July 31, 2019) (TROPOMI, 2019). Rose diagram of daily average wind of the sampling period is shown as inset. Hospital de Caldas weather station (CDIAC, 2019). Symbols: Δ: volcanoes. ●: City of Manizales.

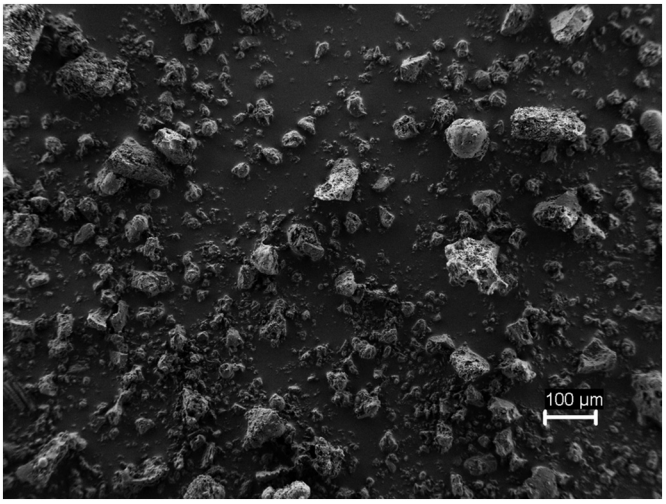

Fig. 5. General road dust FE-SEM view containing spherical, angular, micrometric, and nanometric particles (multiple chemical elements and crystallinity).

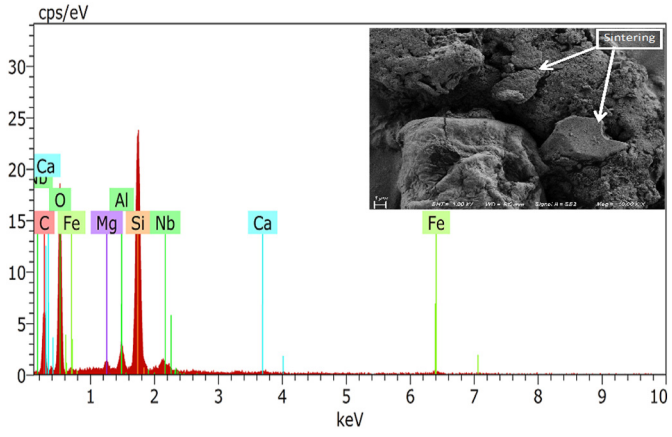

Fig. 6. FE-SEM/EDS image of incipiently welding facies of road dust sample containing Nb near volcano area.

products generated from this date from 600 to 200 years B.P. (before present).

Different studies have reported the geochemical composition of volcanic ash with main elements such as Al, Si, O, Na, Mg, K, Ca, Fe, and Ti in variable concentrations (Cangemi et al., 2017; Lestiani et al., 2018; Lieke et al., 2013). Other important volcanic ash tracers are reported, such as complex and highly porous mixtures of Al-Si-K hydrates (Fig. 7). In some cases, porous particles allow the distinction of kaolinite and different zeolites, with a chemical composition showing a contain of Si, Al, Fe, Ca, K, Mg.

Anthropogenic organic particles of high toxicity, such as fullerenes, carbon nanotubes, graphene, in addition to organometallic complexes containing potential hazardous elements, could be deposited in the pores of such particles. The smallest particles can be released from the pores when they are inhaled generating multiple impacts on health, since they can pass through the respiratory system and enter into the bloodstream, thus reaching the entire body. Therefore, ultra-fine particles of volcanoes can serve as a storage species for highly toxic anthropogenic NPs.

In addition, the porous fine particles collected in this study are always composed of amorphous material and have sulfur in most of the cases (Fig. 6). These particles could generate sulfuric acid in the

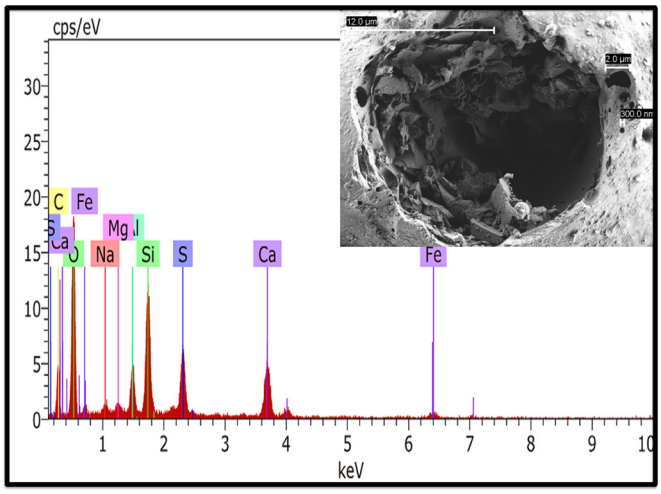

Fig. 7. Example of porous particle with pores that vary from 300 nm to 2 μm. This indicates that such particles can encase other particles, especially those of smaller size.

presence of water (humidity or rain). González and Aristizábal (2012) suggested that conditions of the city, such as the proximity to the volcano and high rainfall, it favors the washing of the atmosphere, dragging the particulate material from the air (phenomenon known as Scavenging), when rainfall they are low can increase the content of pollutants present in the atmosphere in road dust. However, it is important to note that high rainfall can also generate a sweep of road dust.

According to petrographic studies, the plagioclase feldspar (e.g. andesine) is a mineral associated with volcanic zones, as it was described in studies of volcanic evolution of the Mount of Cameroon (located at the ocean-continent boundary of the Cameroon Volcanic Line) using automated electron microprobe analyzer equipped with an EDS (Wembenyui et al., 2020). In two places on the island of Tenerife (the Arenas Negras volcano and the Anaga massif), feldspars were detected by Raman spectroscopy and confirmed by X-ray diffraction and infrared spectroscopy (Lalla et al., 2016). Feldspars were found in microparticles of Himalayan ice cores using SEM/EDS analysis techniques with ATR-FTIR (Malek et al., 2019). FE-SEM/EDS analyzes performed in the present study indicated that, in addition to the presence of plagioclase crystalloclasts (mainly oligoclase-andesine), all samples presented multiple crystals (plagioclase slats, see Fig. 8). Various elongated crystals have not only been detected in the samples near the volcanoes but also regularly in all the samples of this study. These results indicate that ultra-fine volcanic particles are abundant throughout the study area, presenting a serious risk to people's health, especially when they are nanometric and contain potentially toxic elements such as As, Hg, Cd, Pb, among others (e.g. see Fig. 9).

Although magnetite is a mineral that can be derived from several sources (terrestrial crust, building materials, steel industries, vehicular traffic, others), in this study it was detected in more than half of the sampled sites, which allows inferring that the entire study area is impacted by the Nevado del Ruiz volcano. Similarly, elements such as As Hg, Cd, Pb, V, Se, detected by EDS, were also found not only in samples near the Nevado del Ruiz volcano, but also regularly in all study samples (see Fig. 3B). In particular, arsenic, a highly-volatile element with great mobility, is released into the environment through volcanic gases. In this manner, arsenic, in contact with water (e.g. precipitation), is deposited in sediments (Juncos et al., 2016; Rodríguez et al., 2018; Smedley and Kinniburgh, 2002). Studies on the geochemical composition of leachate in ash waters of the Chaitén volcano in Chile have reported high concentrations of major elements such as Cl, S, F, Ca, Mg, Na, K, Si, and Al; trace elements such as As, Pb, P, Fe, Sr, Zn, Mn, and Br; and lower, but significant, contents Ba, Li, Ti, Ni, Nb, and Cu (Ruggieri et al., 2012). Likewise, equivalent results have been reported in other volcanic ash characterization studies (Cangemi et al., 2017; Fernández et al., 2012; Lieke et al., 2013). In contrast, geochemical composition of RD_{10} samples also has influences from anthropogenic sources such as demolition/construction (S, Ca, Sr), industries (Pb, Zn, Mn, Fe, Cl), vehicular exhaust (Elemental Carbon (EC), Organic Carbon (OC), Na, Fe), brake wear (OC, S, Zn), tire wear (As, Rb, K, Zn, Cd), pavement wear (Ba, Zn, Cu, Pb); with semi-spherical, angle, and sub-angled morphology) and burning of biomass (As, Rb, K) (Amato et al., 2009, 2011; Karanasiou et al., 2011; Cheng et al., 2015; Ramirez et al., 2019).

Gypsum found in road dust samples (Fig. 10A) can originate from multiple sources such as construction debris, soil, but also by volcanic reactions in the presence of water. Salammoniac, a mineral detected in this study, serves as volcano tracer (Fig. 10B). Previous studies found that salammoniac results from sublimation around volcanic fumaroles (Gaines et al., 1997). Sulfur is an abundant element in volcano fumaroles, and it is typically found in association with gypsum and salammoniac. Sulfur and salammonia form during gas exhalation and condensation through interaction with surface water, atmospheric gases, and surrounding rocks (Ribeiro et al., 2010). Minerals, such as hematite, zircon (Fig. 10C) and illite (Fig. 10D), present a higher health risk

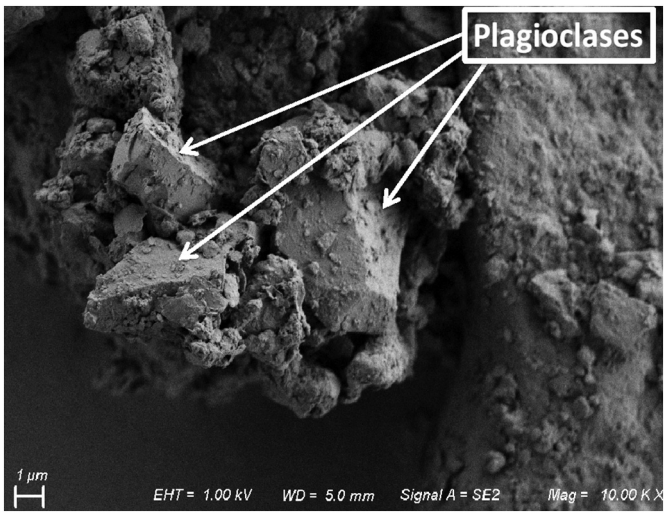

Fig. 8. FE-SEM image of agglomerated of soft and porous hydrous Al—Si particles.

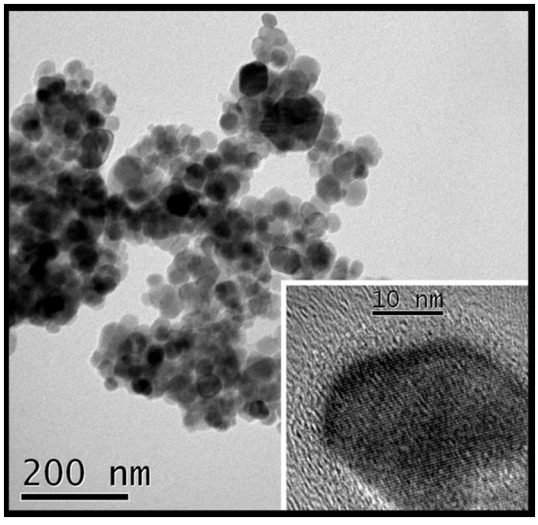

Fig. 9. HR-TEM image of nano-magnetite magnification (containing As and Hg) and amorphous Al-Fe-Si-O-nanoparticles.

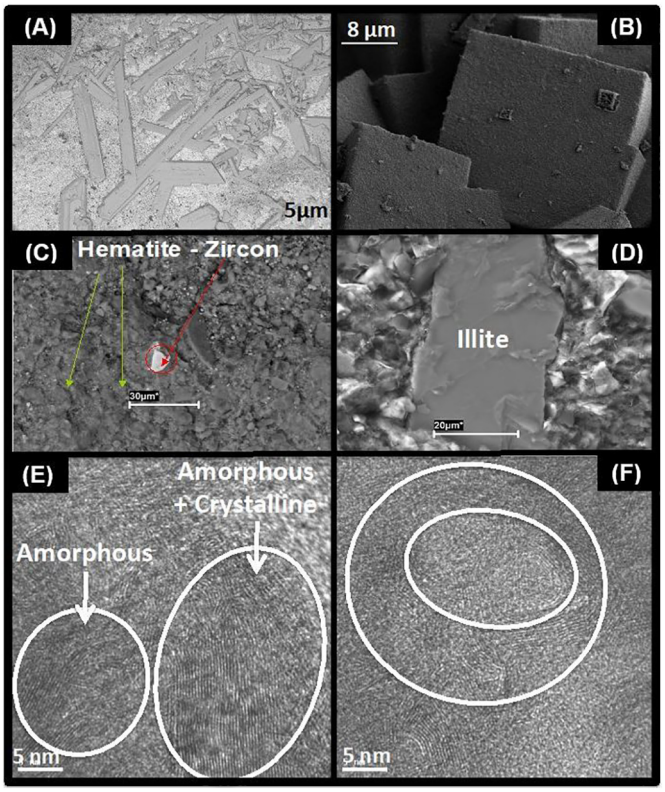

Fig. 10. General FE-SEM illustrations of (A) Gypsum, (B) salammoniac, (C) Hematite aggregate and zircon, (D) Illite; and HR-TEM figures, (E) Amorphous and crystalline carbonaceous materials, (F) Spherical carbon nanotube.

than gypsum (Fig. 10A). Zircon, as well as the monazite and quartz were detected as particles larger than 10 µm, these minerals with high residence time in the environment, and are insolubles in acidic media. In addition, they are minerals of high density, which facilitate their sedimentation and prevent their resuspension. Therefore, in comparison with organic, amorphous ultra-fine (Fig. 10E and 10F), and nanometric particles that contain potentially dangerous elements, they are not considered to be worrisome (Longo et al., 2013; Silva et al., 2020).

Among the collected samples, sites 4, 5, 7, 13, 11, 15, and 17 contained only natural minerals, probably from the soil and/or the volcano. These samples did not show as much occurrence of dangerous elements according to the EDS results (Fig. 3A and B).

4. Conclusions

In this study, the influence of volcanic emissions on road dust (RD_{10}) was analyzed for the first time in Latin America. The advanced microscopic analysis of nanoparticles and ultrafine particles of dust from the roads in Manizales allowed identification of the influence of volcanic emissions from the Nevado del Ruiz volcano. In general, the mineral composition detected was: quartz, mullite, calcite, kaolinite, illite, goethite, magnetite, zircon, monazite, salammoniac (tracer of volcanic sources). Multiple crystals (plagioclase slats - mainly oligoclass-andesine) were observed. Likewise, Si, Al, Fe, Ca, K, Mg and Si—Al with K as complex hydrate, and NPs that contain potentially toxic elements such as As, Hg, Cd, Pb, As, H, Cd, Pb and V were detected. Ultrafine particles of the volcano were present throughout the study area.

Therefore, the importance of conducting more studies that relate the influence of volcanic emissions on road dust in order to establish public air pollution policies that protect human health is reflected, since in the region there are very few or no studies with this approach but many active volcanoes.

These findings are of interest for air quality management, as they highlight the importance of conducting more studies that evaluate the volcanic influence on road dust, and not the influence with parameters such as type of pavement, traffic condition, land use area that is already documented. In addition, complement SEM-EDS image observations with attenuated total reflection: Fourier transform infrared spectroscopy (ATR-FTIR) to identify with certainty in an individual particle its molecular species, functional groups, and crystallinity and specifically identify the type of mineral and their polymorphs.

Declaration of Competing Interest

The authors have not conflict of interest.

Acknowledgments

Special thanks to Fulvio Amato and Xavier Querol from the Spanish Research Council to facilitate the road dust equipment. An acknowledgment to Omar Ramirez for their discussions during the study.

References

Alarcón, E., Murcia, H., Borrero, C., Arnosio, M., 2020. Evidence for welding of a block and ash pyroclastic flow deposit: the case of Cerro Bravo Volcano, Colombia. Bull. Volcanol. 82 (3), 1–14. https://doi.org/10.1007/s00445-019-1334-5.

Alleon, J., Bernard, S., Guillou, C., Marin-Carbonne, J., Pont, S., Beyssac, O., Mckeegan, K., Robert, F., 2016. Molecular preservation of 1.88 Ga Gunflint organic microfossils as a function of temperature and mineralogy. Nature. Communications 7, 11977. https://doi.org/10.1038/ncomms11977.

Amato, F., Pandolfi, M., Viana, M., Querol, X., Alastuey, A., Moreno, T., 2009. Spatial and chemical patterns of PM_{10} in road dust deposited in urban environment. Atmos. Environ. 43 (9), 1650–1659. https://doi.org/10.1016/j.atmosenv.2008.12.009.

Amato, F., Pandolfi, M., Moreno, T., Furger, M., Pey, J., Alastuey, A., Bukowiecki, N., Prevot, A.S.H., Baltensperger, U., Querol, X., 2011. Sources and variability of inhalable road dust particles in three European cities. Atmos. Environ. 45 (37), 6777–6787. https://doi.org/10.1016/j.atmosenv.2011.06.003.

Amato, F., Pandolfi, M., Alastuey, A., Lozano, G., Contreras, J., Querol, X., 2013. Impact of traffic intensity and pavement aggregate size on road dust particles loading. Atmos. Environ. 77, 711–717. https://doi.org/10.1016/j.atmosenv.2013.05.020.

Bergbäck, B., Johansson, K., Mohlander, U., 2001. Urban Metal Flows – a Case Study of Stockholm. Review and Conclusions. Water. Air Soil Pollut. 1, 3–24. https://doi.org/10.1023/A:1017531532576.

Bukowiecki, N., Lienemann, P., Hill, M., Furger, M., Richard, A., Amato, F., Prévôt, A.S.H., Baltensperger, U., Buchmann, B., Gehrig, R., 2010. PM_{10} emission factors for non-exhaust particles generated by road traffic in an urban street canyon and along a freeway in Switzerland. Atmos. Environ. 44 (19), 2330–2340. https://doi.org/10.1016/j.atmosenv.2010.03.039.

Buseck, P.R., Adachi, K., 2008. Nanoparticles in the Atmosphere. Elements 4 (6), 389–394. https://doi.org/10.2113/gselements.4.6.389.

Businger, S., Huff, R., Pattantyus, A., Horton, K., Sutton, A.J., Elias, T., Cherubini, T., 2015. Observing and forecasting Vog Dispersion from Kīlauea Volcano, Hawaii. Bull. Am. Meteorol. Soc. 96 (10), 1667–1686. https://doi.org/10.1175/BAMS-D-14-00150.1.

Campos, A., Aragon, A., Alastuey, A., Galindo, I., Querol, X., 2011. Levels, composition and source apportionment of rural background PM_{10} in Western Mexico (State of Colima). Atmosp. Pollut. Res. 2 (4), 409–417. https://doi.org/10.5094/APR.2011.046.

Cangemi, M., Speziale, S., Madonia, P., D'Alessandro, W., Andronico, D., Bellomo, S., Brusca, L., Kyriakopoulos, K., 2017. Potentially harmful elements released by volcanic ashes: examples from the Mediterranean area. J. Volcanol. Geotherm. Res. 337, 16–28. https://doi.org/10.1016/j.jvolgeores.2017.03.015.

Carn, S., Froyd, K., Anderson, B., Wennberg, P., Crounse, J., Spencer, K., Dibb, J., Krotkov, N., Browell, E., Hair, J., Diskin, G., Sachse, G., 2011. In situ measurements of tropospheric volcanic plumes in Ecuador and Colombia during TC^4. J. Geophys. Res. 116, 1–24. https://doi.org/10.1029/2010JD014718.

Carn, S., Fioletov, V., Mclinden, C., Li, C., Krotkov, N., 2017. A decade of global volcanic SO_2 emissions measured from space. Sci. Rep. 7, 44095. https://doi.org/10.1038/srep44095.

CDIAC [Centro de Datos e Indicadores Ambientales de Caldas], 2019. Datos diarios de velocidad del viento 2019 – Estación meteorológica Hospital de Caldas. http://cdiac.manizales.unal.edu.co/etl-cdiac-app/externalReport/getReportStation.

Chen, H., Kwong, J., Copes, R., Hystad, P., van Donkelaar, A., Tu, K., Brook, J., Goldberg, M., Martin, R., Murray, B., Wilton, A., Kopp, A., Burnett, R., 2017. Exposure to ambient air pollution and the incidence of dementia: a population–based cohort study. Environ. Int. 108, 271–277. https://doi.org/10.1016/j.envint.2017.08.020.

Cheng, Y., Lee, S., Gu, Z., Ho, K., Zhang, Y., Huang, Y., Chow, J., Watson, J., Cao, J., Zhang, R., 2015. $PM_{2.5}$ and $PM_{10-2.5}$ chemical composition and source apportionment near a Hong Kong roadway. Particuology 18, 96–104. https://doi.org/10.1016/j.partic.2013.10.003.

Civeira, M., Pinheiro, R.N., Gredilla, A., de Vallejuelo, S., Oliveira, M.L.S., Ramos, C.G., Taffarel, S.R., Kautzmann, R.M., Madariaga, J.M., Silva, L.F.O., 2016a. The properties of the nano-minerals and hazardous elements: potential environmental impacts of

Brazilian coal waste fire. Sci. Total Environ. 544, 892–900. https://doi.org/10.1016/j.scitotenv.2015.12.026.
Cuesta, A., González, C., Velasco, M., Aristizábal, B., 2018. Distribución espacial de concentraciones de SO_2, NO_x y O_3 en el aire ambiente de Manizales. Revista Internacional de Contaminación Ambiental 34, 489–504. https://doi.org/10.20937/RICA.2018.34.03.11 (in Spanish with English abstract).
Cuesta, A., Wahl, M., Acosta, J., García, A., Aristizábal, B., 2020. Mixing layer height and slope wind oscillation: Factors that control ambient air SO_2 in a tropical mountain city. Sustain. Cities Soc. 52, 101852. https://doi.org/10.1016/j.scs.2019.101852.
Cutruneo, C., Oliveira, M., Ward, C., Hower, J., Brum, I., Sampaio, C., Kautzmann, R., Taffarel, S., Calesso, T., Silva, L., 2014. A mineralogical and geochemical study of three Brazilian coal cleaning rejects: Demonstration of electron beam applications. Int. J. Coal Geol. 130, 33–52. https://doi.org/10.1016/j.coal.2014.05.009.
DANE (Departamento Administrativo Nacional de Estadística), 2019. Censo Nacional de Población y Vivienda 2018. Población ajustada por cobertura. https://www.dane.gov.co/files/censo2018/informacion-tecnica/presentaciones-territorio/190801-CNPV-presentacion-Caldas-Manizales.pdf (in Spanish with English abstract).
EEA (European Environment Agency), 2004. EMEP/CORINAIR Atmospheric Emission Inventory Guidebook, third ed. Technical Report No. 30. European Environmental Agency, Copenhagen, Denmark.
Erazo, D., Londoño, A., Aristizabal, B., 2015. Study of the impact of volcanic fluids on the water resources of the Chinchiná river basin. Manage. Environ. 18 (2), 81–93.
Fernández, J.L., Saavedra, J., Ruggieri, F., Gimeno, D., Perez, F.J., Rodríguez, A., Galindo, G., 2012. Geoquímica de cenizas volcánicas a lo largo de dos transectas en Sudamérica: implicaciones ambientales. Geo-Temas 13, 2–5. http://hdl.handle.net/10261/53751 (in Spanish with English abstract).
Findeter, 2017. Plan Maestro de Movilidad de Manizales. Manizales, Caldas, Colombia.
Gaines, R., Skinner, H., Foord, E., Mason, B., Rosenzweig, A., 1997. Dana's New Mineralogy: The System of Mineralogy of James Dwight Dana and Edward Salisbury Dana. eighth ed. John Wiley & Sons Inc, New York, p. 1819.
González, C., 2017. Dinámica e impacto de emisiones antrópicas y naturales en una ciudad andina empleando un modelo Euleriano de transporte químico on-line. Caso de estudio: Manizales, Colombia. Ph.D thesis. Universidad Nacional de Colombia - sede Manizales, Manizales, Colombia, pp. 234 (in Spanish with English abstract).
González, C., Aristizábal, B., 2012. Acid rain and particulate matter dynamics in a mid-sized Andean city: the effect of rain intensity onion scavenging. Atmos. Environ. 60, 164–171. https://doi.org/10.1016/j.atmosenv.2012.05.054.
Gredilla, A., Fdez-Ortiz de Vallejuelo, S., de Diego, A., Arana, G., Madariaga, J.M., 2014. A new index to sort estuarine sediments according to the contaminant content. Ecol. Indic. 45, 364–370. https://doi.org/10.1016/j.ecolind.2014.04.038.
Gredilla, A., Fdez-Ortiz de Vallejuelo, S., Gomez-Nubla, L., Carrero, J.A., de Leão, F.B., Madariaga, J.M., Silva, L.F., 2017. Are children playgrounds safe play areas? Inorganic analysis and lead isotope ratios for contamination assessment in recreational (Brazilian) parks. Environ. Sci. Pollut. Res. 24, 333–345. https://doi.org/10.1007/s11356-017-9831-6.
Grigoratos, T., Martini, G., 2015. Brake wear particle emissions: a review. Environ. Sci. Pollut. Res. 22, 2491–2504. https://doi.org/10.1007/s11356-014-3696-8.
Harrison, R.M., Stedman, J., Derwent, D., 2008. New Directions: why are PM_{10} concentrations in Europe not falling? Atmos. Environ. 42 (3), 603–606. https://doi.org/10.1016/j.atmosenv.2007.11.023.
Hussein, T., Johansson, C., Karlsson, H., Hansson, H.-C., 2008. Factors affecting non tail pipe aerosol particle emissions from paved roads: On-road measurements in Stockholm Sweden. Atmos. Environ. 42 (4), 688–702. https://doi.org/10.1016/j.atmosenv.2007.09.064.
Juncos, R., Arcagni, M., Rizzo, A., Campbell, L., Arribére, M., Guevara, S.R., 2016. Natural origin arsenic in aquatic organisms from a deep oligotrophic lake under the influence of volcanic eruptions. Chemosphere 144, 2277–2289. https://doi.org/10.1016/j.chemosphere.2015.10.092.
Karanasiou, A., Moreno, T., Amato, F., Lumbreras, J., Narros, A., Borge, R., Tobías, A., Boldo, E., Linares, C., Pey, J., Reche, C., Alastuey, A., 2011. Road dust contribution to PM levels – Evaluation of the effectiveness of street washing activities by means of Positive Matrix Factorization. Atmos. Environ. 45 (13), 2193–2201. https://doi.org/10.1016/j.atmosenv.2011.01.067.
Kioumourtzoglou, M., Schwartz, J., James, P., Dominici, F., Zanobetti, A., 2016. $PM_{2.5}$ and Mortality in 207 US Cities: Modification by Temperature and City Characteristics. Epidemiology 27 (2), 221–227. https://doi.org/10.1097/EDE.0000000000000422.
Kumar, P., Fennell, P., Hayhurst, A., Britter, R., 2009. Street versus rooftop level concentrations of fine particles in a Cambridge street canyon. Bound.-Layer Meteorol. 131, 3–18. https://doi.org/10.1007/s10546-008-9300-3.
Kumar, P., Morawska, L., Birmili, W., Paasonen, P., Hu, M., Kulmala, M., Harrison, R., Norford, L., Britter, R., 2014. Ultrafine particles in cities. Environ. Int. 66, 1–10. https://doi.org/10.1016/j.envint.2014.01.013.
Labrada, G., Aragon, A., Campos, A., Castro, T., Amador, O., Villalobos, R., 2012. Chemical and morphological characterization of $PM_{2.5}$ collected during MILAGRO campaign using scanning electron microscopy. Atmos. Pollut. Res. 3 (3), 289–300. https://doi.org/10.5094/APR.2012.032.
Laj, P., Boutron, C., 1990. Trace elements in snow deposited at Nevado del Ruiz volcano, Colombia. J. Volcanol. Geotherm. Res. 42, 89–100. https://doi.org/10.1016/0377-0273(90)90071-M.
Lalla, E., Lopez-Reyes, G., Sansano, A., Arranz, A., Martínez-Frías, J., Medina, J., Rull, F., 2016. Raman-IR vibrational and XRD characterization of ancient and modern mineralogy from volcanic eruption in Tenerife Island: Implication for Mars. Geosci. Front. 7 (4), 673–681. https://doi.org/10.1016/j.gsf.2015.07.009.
Lepot, K., Addad, A., Knoll, A., Wang, J., Troadec, D., Béché, A., Javaux, E., 2017. Iron minerals within specific microfossil morphospecies of the 1.88 Ga Gunflint Formation. Nat. Commun. 8, 1–11. https://doi.org/10.1038/ncomms14890.
Lestiani, D., Apryani, R., Lestari, L., Santoso, M., Hadisantoso, E., Kurniawati, S., 2018. Characteristics of Trace elements in Volcanic ash of Kelud Eruption in East Java, Indonesia. Indian J. Chem. 18 (3), 457–463. https://doi.org/10.22146/ijc.26876.
Lieke, K., Kristensen, T., Korsholm, U., Sørensen, J., Kandler, K., Weinbruch, S., Ceburnisd, D., Ovadnevaite, J., O'Dowd, C., Bilde, M., 2013. Characterization of volcanic ash from the 2011 Grímsvötn eruption by means of single-particle analysis. Atmos. Environ. 79, 411–420. https://doi.org/10.1016/j.atmosenv.2013.06.044.
Longo, B.M., 2013. Adverse Health Effects Associated with increased activity at Kīlauea Volcano: a Repeated Population-based survey. ISRN Public Health 2013, 475962. https://doi.org/10.1155/2013/475962.
Malek, A., Eom, H., Hwang, H., Hur, S., Hong, S., Hou, S., Ro, C., 2019. Single particle mineralogy of microparticles from Himalayan ice-cores using SEM/EDX and ATR-FTIR imaging techniques for identification of volcanic ash signatures. Chem. Geol. 504, 205–215. https://doi.org/10.1016/j.chemgeo.2018.11.010.
Manizales Cómo Vamos, 2019. Informe calidad de vida Manizales 2019. ISSN 2389-9514. http://manizalescomovamos.org/wp-content/uploads/2019/09/Calidad_de_vida_2019_compressed.pdf.
Mantovani, L., Tribaudino, M., Solzi, M., Barraco, V., De Munari, E., Pironi, C., 2018. Magnetic and SEM-EDS analyses of *Tilia cordata* leaves and PM_{10} filters as a complementary source of information on polluted air: results from the city of Parma (Northern Italy). Environ. Pollut. 239, 777–787. https://doi.org/10.1016/j.envpol.2018.04.055.
Onat, B., Sahin, U.A., Akyuz, T., 2013. Elemental characterization of $PM_{2.5}$ and PM_1 in dense traffic area in Istanbul, Turkey. Atmos. Pollut. Res. 4 (1), 101–105. https://doi.org/10.5094/APR.2013.010.
Pachón, J.E., Vanegas, J., Saavedra, C., Amato, F., Silva, L.F.O., Blanco, K., Chaparro, R., Casas, O., 2020. Evaluation of factors influencing road dust loadings in a Latin American urban center. J. Air & Waste Manag. Assoc. https://doi.org/10.1080/10962247.2020.1806946.
Parnell, R., Burke, K., 1990. Impacts of acid emissions from Nevado del Ruiz volcano, Colombia, on selected terrestrial and aquatic ecosystems. J. Volcanol. Geotherm. Res. 42, 69–88. https://doi.org/10.1016/0377-0273(90)90070-V.
Querol, X., Alastuey, A., Rodríguez, S., Plana, F., Mantilla, E., Ruiz, C.R., 2001. Monitoring of PM_{10} and $PM_{2.5}$ ambient air levels around primary anthropogenic emissions. Atmos. Environ. 35 (5), 848–858. https://doi.org/10.1016/S1352-2310(00)00387-3.
Ramírez, O., Verdona, A., Amato, F., Moreno, T., Silva, L., de la Rosa, J., 2019. Physicochemical characterization and sources of the thoracic fraction of road dust in a Latin American megacity. Sci. Total Environ. 652, 434–446. https://doi.org/10.1016/j.scitotenv.2018.10.214.
Ribeiro, J., Flores, D., Ward, C., Silva, L.F.O., 2010. Identification of nanominerals and nanoparticles in burning coal waste piles from Portugal. Sci. Total Environ. 408, 6032–6041. https://doi.org/10.1016/j.scitotenv.2010.08.046.
Ribeiro, J., Daboit, K., Flores, D., Kronbauer, M., Silva, L., 2013a. Extensive FE-SEM/EDS, HR-TEM/EDS and ToF-SIMS studies of micron- to nano-particles in anthracite fly ash. Sci. Total Environ. 452-453, 98–107. https://doi.org/10.1016/j.scitotenv.2013.02.010.
Ribeiro, J., Taffarel, S.R., Sampaio, C.H., Flores, D., Silva, L.F.O., 2013b. Mineral speciation and fate of some hazardous contaminants in coal waste pile from anthracite mining in Portugal. Int. J. Coal Geol. 109-110, 15–23. https://doi.org/10.1016/j.coal.2013.01.007.
Rodríguez, P.F., Shruti, V.C., Jonathan, M.P., Martinez, E., 2018. Metal concentrations and their potential ecological risks in fluvial sediments of Atoyac River basin, Central Mexico: Volcanic and anthropogenic influences. Ecotoxicol. Environ. Saf. 148, 1020–1033. https://doi.org/10.1016/j.ecoenv.2017.11.068.
Ruggieri, F., Fernandez, J., Saavedra, J., Gimeno, D., Polanco, E., Amigo, A., Galindo, G., Caselli, A., 2012. Contribution of volcanic ashes to the regional geochemical balance: the 2008 eruption of Chaiten volcano, Southern Chile. Sci. Total Environ. 425, 75–88. https://doi.org/10.1016/j.scitotenv.2012.03.011.
Saikia, B.K., Saikia, J., Rabha, S., Silva, L.F.O., Finkelman, R., 2018. Ambient nanoparticles/nanominerals and hazardous elements from coal combustion activity: Implications on energy challenges and health hazards. Geosci. Front. 9 (3), 863–875. https://doi.org/10.1016/j.gsf.2017.11.013.
Schäfer, K., Thomas, W., Peters, A., Ries, L., Obleitner, F., Schnelle-Kreis, J., Birmili, W., Diemer, J., Fricke, W., Junkermann, W., Pitz, M., Emeis, S., Forkel, R., Suppan, P., Flentje, H., Gilge, S., Wichmann, H.E., Meinhardt, F., Zimmermann, R., Weinhold, K., Soentgen, J., Münkel, C., Freuer, C., Cyrys, J., 2011. Influences of the 2010 Eyjafjallajökull volcanic plume on air quality in the northern Alpine region. Atmos. Chem. Phys. 11, 8555–8575. https://doi.org/10.5194/acp-11-8555-2011.
SGC [Servicio Geológico Colombiano], 2015. Mapa de amenaza volcánica del Volcán Nevado del Ruiz, v3. https://www2.sgc.gov.co/sgc/volcanes/VolcanNevadoRuiz/Paginas/Mapa-amenaza.aspx.
SGC [Servicio Geológico Colombiano], 2019. Boletín semanal de actividad del volcán Nevado del Ruiz. Manizales, Caldas. Dirección de Geoamenazas.
Silva, L., Pinto, D., Neckel, A., Oliveira, M.L.S., Sampaio, C., 2020. Atmospheric nanocompounds on Lanzarote Island: Vehicular exhaust and igneous geologic formation interactions. Chemosphere 254, 126822. https://doi.org/10.1016/j.chemosphere.2020.126822.
Smedley, P.L., Kinniburgh, D.G., 2002. A review of the source, behavior and distribution of arsenic in natural waters. Appl. Geochem. 17 (5), 517–568. https://doi.org/10.1016/S0883-2927(02)00018-5.
Sörme, L., Bergbäck, B., Lohm, U., 2001. Goods in the Anthroposphere as a Metal Emission Source a Case Study of Stockholm, Sweden. Water, Air Soil Pollut. 1, 213–227. https://doi.org/10.1023/A:1017516523915.
Stafoggia, M., Faustini, A., 2018. Chapter 3 - Impact on Public Health—Epidemiological Studies: A Review of Epidemiological Studies on Non-Exhaust Particles: Identification of Gaps and Future needs. In: Amato, F. (Ed.), Non-Exhaust Emissions. Academic Press, London, pp. 67–88 https://doi.org/10.1016/B978-0-12-811770-5.00003-0.

TROPOMI [TROPOspheric Monitoring Instrument], 2019. Satellite image of the volcanic ash emission, trajectory, and height of the SO_2 column – Nevado del Ruiz volcano. Colombia. http://www.tropomi.eu/data-products/level-2-products

UNAL [Universidad Nacional de Colombia – sede Manizales]., CORPOCALDAS [Corporación Autónoma Regional de Caldas], 2019. Aplicación de herramientas de simulación atmosférica en el estudio de la calidad del aire en Manizales. Convenio Interadministrativo 107–2018. Colombia, Manizales, Caldas, p. 233.

Velasco, M., 2015. Evaluación de la concentración y caracterización preliminar del PM_{10} en la ciudad de Manizales. Master's thesis. Universidad del Valle. Santiago de Cali, Colombia. 105 pp.

Wembenyui, E., Collerson, K., Zhao, J., 2020. Evolution of Mount Cameroon volcanism: Geochemistry, mineral chemistry and radiogenic isotopes (Pb, Sr, Nd). Geosci. Front. https://doi.org/10.1016/j.gsf.2020.03.015 corrected proof.

WHO [World Health Organization], 2016. World health statistics 2016: monitoring health for the SDGs, sustainable development goals. E-ISBN 9789240695696. https://www.who.int/gho/publications/world_health_statistics/2016/en/.